Thermal Fluids Analysis Workshop 2006 (TFAWS 2006)
University of Maryland, College Park, MD
August 7-11, 2006

TFAWS06-1015:
Thermal Analysis of a Sea Level Launched Hypersonic Projectile

A.A. Mabbett
Naval Surface Warfare Center Dahlgren
Dahlgren, VA

ABSTRACT

Hypersonic launch of a projectile in the low earth atmosphere presents several engineering obstacles. Structural survivability due to acceleration and thermal load management are significant difficulties. An extreme thermal environment on a relatively small object increases the complexity of the thermal protection system design. A baseline thermal model can assist with early designs and trade studies. In a previous study presented at TFAWS 2005 semi-empirical codes were used to obtain a preliminary full up thermal response. Over the past year numerous codes have been utilized to increase the fidelity of the previous aeroheating study while including ablation effects. The study presented will discuss some of the capabilities and limitations of these codes as well as preliminary design results.

INTRODUCTION

Over the last few decades, significant advances have occurred in support of electromagnetic launch (EML). The US Navy is currently considering an EM Railgun concept as a future long range naval weapons system. Preliminary studies have shown such a system will have the capability to launch a projectile upwards of 2.5 km/s over 200 nautical miles. Significant challenges exist in the design of a projectile system capable of withstanding this severe launch environment.[1]

HYPERSONIC LAUNCH CONDITIONS

The purpose of this analysis is to gain a better understanding of the thermal environment experienced by the EM Railgun hypersonic round as well as the capabilities and limitations of various aeroheating codes. For configuration ease a general cone shaped projectile was used with a nose tip radius of 0.125", control surfaces were not considered for this study. [See Figure 1]. As mentioned previously, the launch occurs at sea level with an initial velocity of 2.5 km/s, approximately Mach 7.5. For design margin Mach 8 launch was studied at various quadrant elevations (QE – i.e. gun elevation angle).

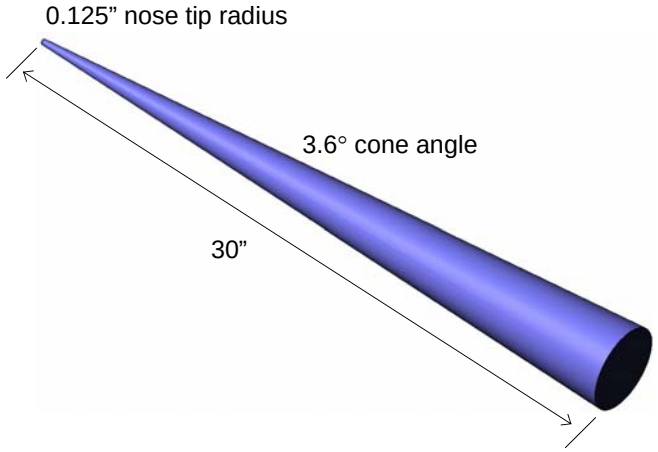

FIGURE 1: HYPERSONIC ROUND AIRFRAME

AEROHEATING CODES

BLUNTY (SNL)

BLUNTY was originally developed in the late 1960's at Sandia National Laboratories in order to capture the aerodynamic heating rates for standard sphere-cone geometries. The procedure uses curve fits to shock shape and pressure distributions obtained from tables defined by runs of the NASA AMES Flow Field (NAFF) code.[2] The boundary layer edge properties are determined via a streamtube mass balancing technique which couples the inviscid flow field to a boundary layer mass flux correlation. Both ideal gas and thermodynamic equilibrium air models are available. Heat transfer rates are calculated based on Fay and Riddell (stagnation), Kemp, Rose, and Detra (laminar), and a modified Rose, Probstein, and Adams (turbulent).

Sandia One-Dimensional Direct and Inverse Thermal Code (SODDIT) (SNL)

SODDIT was developed by Sandia National Labs to account for in depth conduction and ablation effects of reentry vehicles. The code is set up to accept enthalpy based aeroheating decks from codes such as BLUNTY to be applied as boundary conditions. With the heat flux boundary conditions applied a one dimensional heat conduction solution is obtained. The boundary conditions are applied consistently over the entire surface depending on the geometry option selected. SODDIT can model three geometric options – flat plate, curved surface (i.e. cylinders and cones), or

sphere. Depending on the geometry of the object being modeled one of the three options should be acceptably representative. Ablation effects are accounted for using the Q* method (melting ablation only). Q* is essentially the amount of material loss per unit of energy. Once the material reaches the melt temperature it begins to ablate at a rate based on the Q* value. The higher the Q* value the more energy is required to ablate a given mass.

MAGIC Suite (SNL)

The MAGIC suite of tools is essentially a front end run stream that executes a nose tip code, an inviscid afterbody code, and a boundary layer code. The default nose tip code, General Electric Two-Dimensional Inviscid Transonic, solves the non-conservative form of the unsteady Euler equations in a spherical coordinate system using a radial grid.[3]

SANDia Inviscid Afterbody Code (SANDIAC) is an extensively updated version of the General Electric Three Dimensional Inviscid Supersonic Code. Both the non-conservative and conservative forms of the Euler equations are solved in a cylindrical coordinate system.

Lastly, in order to obtain the boundary layer solution the Hypersonic Integral Boundary Layer Analysis of Reentry Geometries (HIBLARG) is used. The code solves the integral forms of the momentum and energy equations along the inviscid streamlines for a three dimensional flowfield.[4] Both ideal gas and equilibrium air models are available. The code can predict aerodynamics, aeroheating, and flow-field properties for complex reentry vehicle configurations.

MAGIC was not used for this particular study but was included for academic completeness.

ABRES Shape Change Code (ASCC86) (SNL)

ASCC was developed in the late 1970's to capture the axisymmetric shape change phenomena and material response of reentry vehicle nose tips. Since it's release ASCC has continuously undergone improvements and expansions to incorporate the advances in reentry technology.

Surface pressure distribution in ASCC86 is broken into three regimes. The region from stagnation to sonic point along the body is region one. Sonic point to aft body shoulder is region two. Points downstream of the shoulder are considered region three. For the subsonic region one the Dahm-Anderson extension of the Love correlation is used. Region two uses modified Newtonian theory. Region three is a correlation developed at Aerospace Corporation based off blast wave theory (for Mach 5 and greater flow). Below Mach 5 Region two is extended aftward. These pressure distributions and shock shape predictions are used much like in BLUNTY to calculate the heating rates with some minor modifications. Predominantly the heating rates are computed with the Momentum/Energy Integral Technique (MEIT). Please refer to the ASCC technical reports for more details including high altitude heating.[5]

The boundary conditions calculated are then applied to geometric grid to capture the two dimensional material response and ablation. (See Figure 7) Ablation is computed using an equilibrium chemistry model. This enables materials such as carbon-carbon to be analyzed. Also included is a basic particle impact model – though from brief examination not as thorough as ATAC05 particle module.

ATAC05

ITT grew the Aeroheating and Thermal Analysis Code (ATAC) from its predecessor ABRES Shape Change Code. As noted previously ASCC86 used by Sandia and ATAC have a similar heritage but over the years various modifications and tweaks have distinguished the two. ATAC was developed to analyze non-axisymmetric, three-dimensional nose tip shape change due to angle of attack and/or non-uniform material roughness.[6] ATAC05 in particular had been modified to also now include the Charring Material Thermal Response and Ablation (CMA) procedure.

ATAC05 is an extremely useful tool with the ability to perform a multitude of physical phenomena in an efficient manner. The code is one of the only codes that have an extensive particle impact model to incorporate erosion effects.

Currently the code is still driven via unformatted input decks however there is an ongoing effort by ITT and AMRDEC to incorporate graphical user interface geometry builders and post processors.

RESULTS AND DISCUSSION

The intent of this study is to systematically increase the level of fidelity of the analysis using various tools as described previously and more importantly develop an understanding of the capabilities and limitations of the codes. Past papers presented have discussed the use of basic heat transfer correlations – such as semi-infinite solid estimates – as well as the use of basic aero-prediction tools (AP05). These past studies had looked at the heat transfer boundary conditions as well as overall system thermal response. No ablation or erosion effects were considered. By incorporating more specialized codes into the analyses these effects can now be addressed.

BLUNTY/SODDIT, from Sandia National Laboratories, is the first increment in fidelity of this study. The intent of BLUNTY/SODDIT is to predict aerodynamic heating boundary conditions and the resulting material response in an accurate and efficient manner. These tools together make up an excellent engineering tool to perform numerous quick trade studies.

BLUNTY uses experimental data to establish shock and pressure parameters. For cases that fall within this realm of available data, BLUNTY tends to predict aeroheating conditions very well. However, exercising the code outside the intended geometries can introduce significant uncertainty for off stagnation point calculations (smallest cone angle data is 5°). Due to the normality of the shock at the stagnation point BLUNTY, using Fay and Riddel theory, accurately predicts stagnation point heat transfer rates regardless of the geometry.

The BLUNTY output directly feeds into SODDIT as boundary conditions for a one-dimensional material response analysis. For

most cases a one-dimensional conduction code is sufficient for material response trade studies however for highly conductive materials as well as some of the smaller geometries the multi-dimensional effects may be considerable. SODDIT makes use of the Q* ablation method as mentioned earlier. There are numerous materials of interest that do not behave according to this model and therefore cannot be analyzed in SODDIT. Lastly, SODDIT has the capability to analyze three geometric orientations – flat plate, curved surface, and sphere. Essentially the user defines the thickness of the layer and the material properties. SODDIT applies the boundary conditions to the entire surface. As one can imagine the flat plate approach is less stringent whereas the sphere assumes the heat transfer over the entire surface resulting in the most conservative estimates of temperature (and ablation). In larger geometric systems these approaches can predict within reason a good estimate of material response. However, in a system such as the hypersonic round none of the approaches truly replicates the geometry (0.125" nose tip, 3.6° cone angle). A sphere grossly under-represents the thermal mass of the system whereas the flat plate geometry results in extremely thin layers in order to capture the system mass.

Regardless of the limitations, the tool set of BLUNTY/SODDIT provides an excellent means to run trade studies in order to establish trends and provide insight into the problem at hand. One of the initial studies performed was to compare the cold wall heat flux at the stagnation point for the various trajectories. Figure 2 is a plot of the BLUNTY cold wall heat flux values for various quadrant elevation (QE) launches at Mach 8 for the first fifty seconds. Figure 3 extends the plot to the entire time of flight.

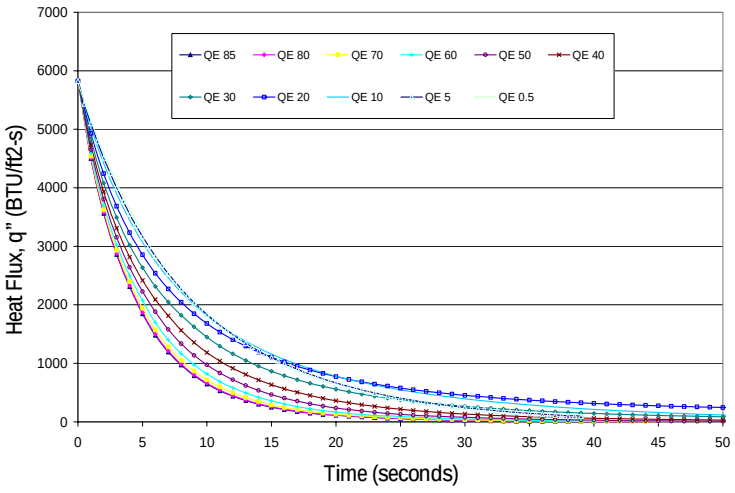

FIGURE 2: BLUNTY COLD WALL HEAT FLUX (50 SEC)

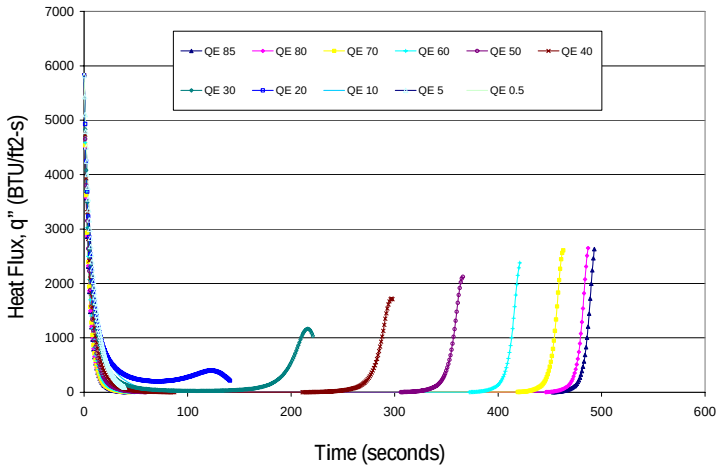

FIGURE 3: BLUNTY COLD WALL HEAT FLUX (FULL)

Figures 2 and 3 are plots of the cold wall heat flux values from BLUNTY over the first few seconds of flight as well as the entire trajectory. The intent of these plots is to show how similar each trajectory is initially but over the full time of flight, each trajectory experiences varying degrees of heat flux. From the plots one can deduce that the area under the curve should represent the most severe case in terms of ablation however it is not clear whether this is also the worst thermal soak scenario. The twenty degree launch angle case is expected to have the most material loss from ablation due to the integrated heat load but since the flight is relatively short it may not have enough time to propagate that heat rearward into the round. The longer flight times that retain considerable heat loads are more likely the most severe thermal soak cases. Lastly a closer look at the cold wall heat flux calculations from BLUNTY compared to that done using an in-house methodology as well as the Detra correlation. Only the first few seconds were plotted to show some small variation but as expected all three match very well.

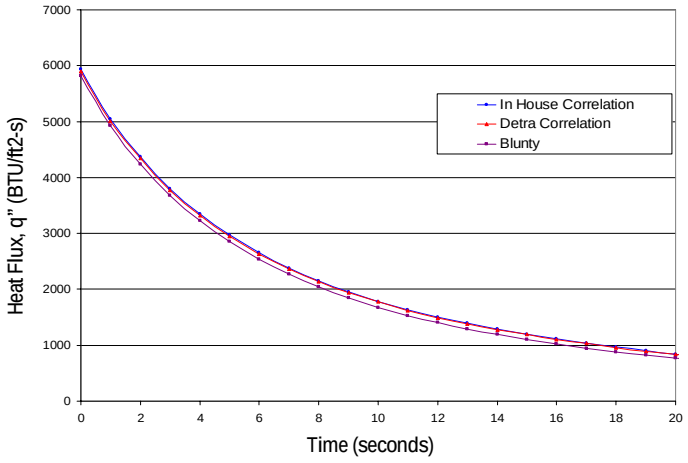

FIGURE 4: BLUNTY, IN-HOUSE, DETRA COMPARISON

SODDIT has limited material options that are of interest in this particular application. In particular, due to the nature of the projectile heavy refractory metals are very beneficial for both flight stability and penetration mechanics. Pure tungsten was used for an initial study primarily to determine approximate maximum temperatures experienced at the stagnation point. To be conservative, a sphere geometry was used with a radius

matching that of the nose tip (0.125”). The longest range case was analyzed (QE = 50°).

Figure 5 plots the results at various depths into the surface. Since the sphere is a mere quarter of an inch diameter there is virtually no difference through the thickness. The maximum temperature predicted by BLUNTY/SODDIT is approximately 5200 °R (2888 K) which occurs less than a second after launch. Notice the overall temperature profile spikes at launch and quickly dissipates as the projectile slows and increases in altitude. Upon reentry there is some additional heating but not nearly as severe as upon launch. Pure tungsten has an extremely high melting temperature, as do most refractory metals. Since the mode of ablation in these materials is melting ablation none will occur for the pure tungsten since the maximum temperature experienced is below the melting point (6611 °R, 3672 K). Unfortunately this is not the case in the real world. Tungsten undergoes a very slow oxidation process at room temperature. Above 1400 °R (777K), the process significantly increases. When the material reaches temperatures in excess of 2600 °R (1445K) the oxide sublimates as rapidly as it forms thus resulting in substantial material loss. Figure 6 shows the amount of material loss expected during the long range case for a more realistic tungsten tip.

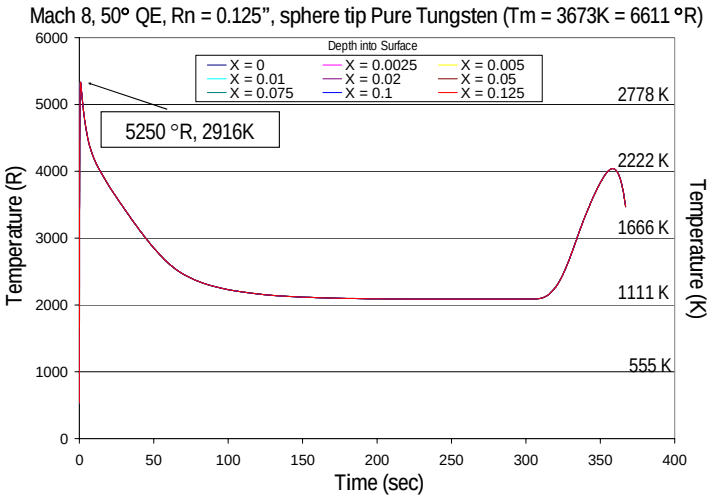

FIGURE 5: BLUNTY/SODDIT THERMAL RESPONSE

These results from BLUNTY/SODDIT are not intended to be the final word on the analyses but more an insight into some of the concerns and challenges this analysis will experience. The severe thermal shock environment is unlike that of any other system. The temperatures expected have been seen before in other systems but the material solutions are not trivial. Lastly, considerable attention needs to be directed towards understanding how materials behave at these temperatures, pressures, and shock.

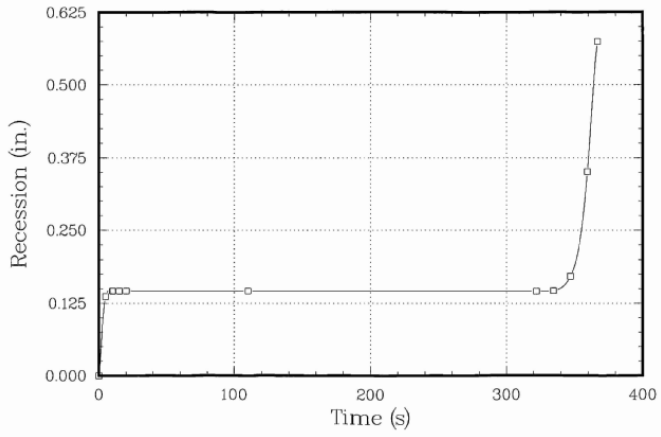

FIGURE 6: TUNGSTEN OXIDE RECESSION, M8, RN = 0.125”, FLAT PLATE

The MAGIC suite of tools was not used in this portion of the analysis. It is intended to provide much more accurate boundary condition results for general geometries than BLUNTY. It will be discussed later where MAGIC will come into play for future efforts. This effort focused more heavily on nose-tip material response and stagnation point heating. Future efforts will examine thermal soak effects more rigorously.

ASCC86 is a self contained aeroheating and material response code. ASCC takes a very similar approach to solving the boundary conditions as BLUNTY and MAGIC however the material response code incorporates two dimensional effects as well with more realistic geometric modeling. ASCC and ATAC05 both evolved out of the same code and are two of the most widely used tools in this community. Both codes have exceptional capabilities as well as some limitations that will be discussed.

Both ASCC86 and ATAC05 are driven via input decks. In the current available release (as of April 2006) ATAC05 was driven entirely by the input deck. One major upgrade from the original code is the formatting restrictions are not as stringent regarding the placement in the columns. There is some working currently being undertaken by both AMRDEC and ITT to integrate more GUI based deck drivers. With the planned upgrades ATAC05 will be an exceptionally efficient code.

Rather than attempting to develop GUI based interfaces Sandia National Labs has developed an interactive script which prompts the user for the input necessary to run the code. As an added benefit the user has a high level of control on the input deck as well as given tips and suggestions on defining various parameters.

ASCC utilizes two overlapping, orthogonal coordinate systems – a moving body-oriented coordinate system which covers the heated surface layer and a fixed cylindrical system covering the computational domain. A finite difference approach is used in both regions however the heated layer region uses an implicit scheme whereas the computational domain is explicit. Essentially the heated layer captures the surface effects while the computational domain calculates the temperature response of the material. (See Figure 7)[5]

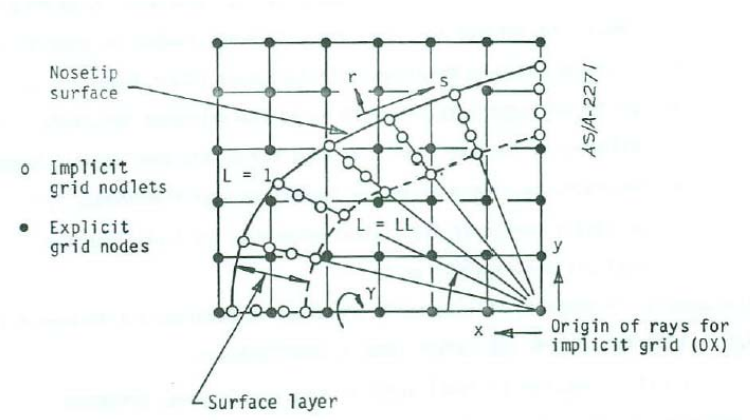

FIGURE 7: ASCC IMPLICIT AND EXPLICIT GRID[10]

The implicit gridding scheme requires a single point origin in the explicit grid at which the grid rays emanate from. This scheme has been well validated and verified for numerous applications and larger scale bodies but there are some inherent risks with smaller more slender systems. A basic assumption with finite difference formulation in the implicit region is that the lateral diffusion term is small compared with the normal diffusion term. This in turn requires that the rays need to be as ortho-normal to the surface as possible. There have been some corrections built in to ASCC however extreme lack of orthogonality causes significant numerical instabilities. When the origin is placed too close to the nose tip the rays become highly skewed invalidating the orthogonality requirement. Also, in extreme cases the surface recession can actually overtake the origin causing the grid to be invalid. On the other hand placing the origin too far rearward can cause a geometric cusp in the grid causing instabilities as well. ASCC86 has for the most part resolved the cusp issue by implementing a scheme to use vertical lines past the origin to ensure orthogonality. There are some general "rules of thumb" suggested for selecting the origin but at times, particularly in the more complex geometries an iterative approach must be taken.

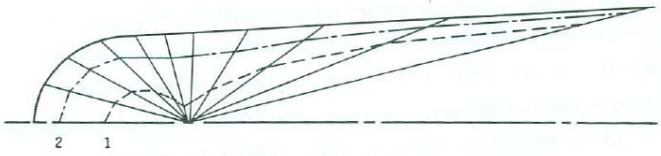

FIGURE 8: HIGHLY SKEWED GRID DUE TO THICK SURFACE LAYER AND ORIGIN LOCATION[10]

In this particular analysis the skewness limitation was encountered often. The design nose tip, 0.125 inch, was much too small to establish an orthogonal grid and the code would discontinue when it could not converge to a solution. The most promising approach was when the origin was moved close to the tip thus setting up a more orthogonal grid however only a few time steps into the solution and the ablation effects would surpass the origin. Systematically various parameters were tweaked in an attempt to converge to a solution but to no avail. The last attempt was to slowly increase the nose tip radius until finally convergence would be reached. The smallest nose tip radius for this geometry converged by ASCC was 0.20 inch. With this in mind all the results obtained are for this nose tip radius and not the design nose tip. It would be expected that a slight increase in ablation and maximum heat flux will be seen for the smaller nose tip.

With the improved modeling capability of ASCC versus BLUNTY/SODDIT a more robust look was needed for various configurations – as well as looking at more suitable material candidates such as carbon-carbon. Many in the community assume that the direct fire, low quadrant elevation (QE), trajectories will be the most severe temperatures and ablation rates. For this reason a QE of 0.5 degree was analyzed as well as the 20, 50, and 85 degree cases. The following figures show the thermal history and ablation recession histories. Notice the thermal histories have some oscillation during the solution that eventually converge to a more behaved trace. This variation is on the order of 8% at most which is acceptable.

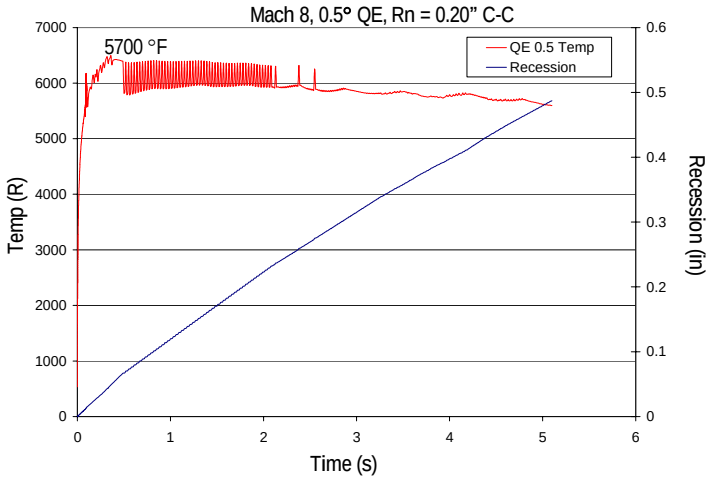

FIGURE 9: ASCC, MACH 8, QE 0.5, C-C

In general all trajectories experienced the same approximate maximum temperature, 6200 °R (3444K), which is expected. Due to the nature of the flight – Mach 8, sea level launch – the heat flux on the round is greatest right at launch. The maximum nose tip temperature experienced is shortly after launch, numerically on the order of a tenth of a second. More so in reality the maximum temperatures would be almost instantaneous. It is interesting to note that 6200 °R (3444 K) is for all intents and purposes approximate. However, this number is higher than the theoretical maximum fluid temperature. The best explanation for this effect – which was not seen in tungsten or other refractory metals – is that carbon-carbon ablation is an exothermic reaction. Therefore the ablation of the material actually results in additional heat generated, much like the use of coal in a barbecue.

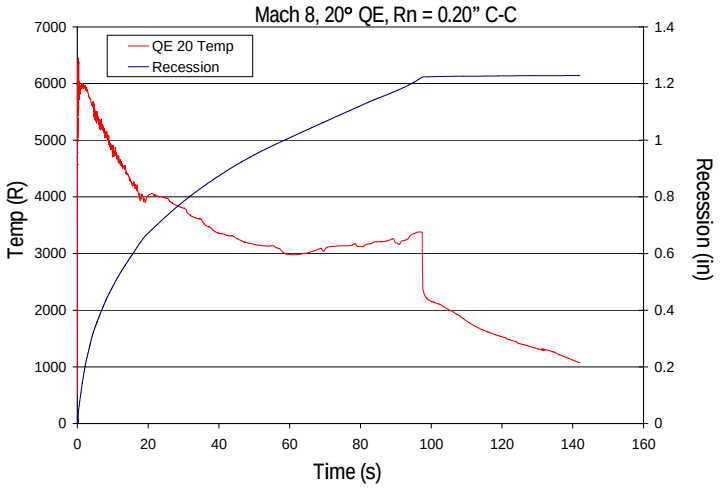

FIGURE 10: ASCC, MACH 8, QE 20, C-C

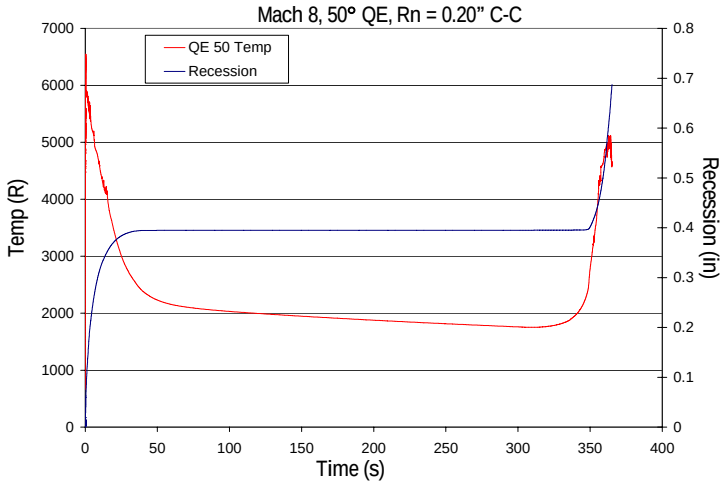

FIGURE 11: ASCC,MACH 8, QE 50, C-C

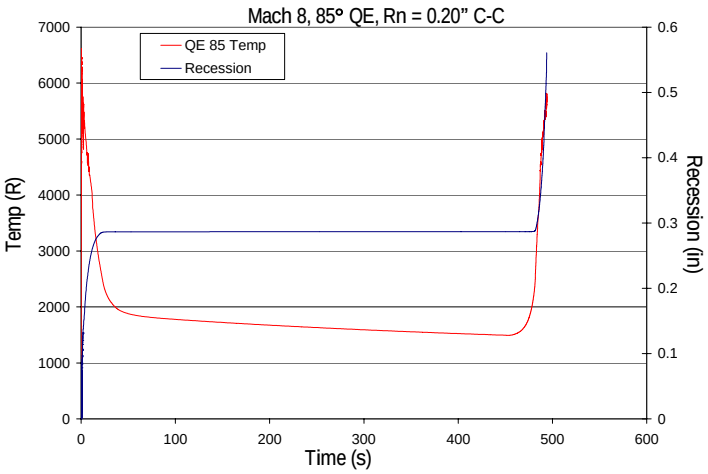

FIGURE 12: ASCC,MACH 8, QE 85, C-C

The RV community has flown carbon-carbon nose tips to the temperatures in flight demonstrations as well as exposed them to similar high pressure and shear stresses. The major difference however is the time to which the maximum forces are reached. RVs enter from extreme altitudes with no heating or pressure effects. Gradually the material begins to experience the shear forces and the heat loads. In a sea level launched application there is no "gradual". At muzzle exit the nose tip is hit instantaneously with extreme temperatures and pressures. The resulting thermal shock and shear forces could easily rip apart materials. Current facilities cannot replicate such environments. Until these rounds can be fired at these speeds in a sea level environment the best that can be done at the present is to assume that the data collected from arc jets, laser tests, and light gas guns can be extrapolated to this regime.

After muzzle exit and reaching maximum temperatures the remaining temperature profile and recession is entirely dependent on the trajectory – neglecting particle impact erosion. Essentially the trajectory with the lowest altitude and highest velocity will maintain the higher heat flux values. This reason alone is why in fact the direct fire, i.e. entire sea level flight, is less severe and a mid range trajectory will be the most stringent.

The direct fire trajectory, QE 0.5 degrees, hits a peak temperature of roughly 6200 °R (3444 K). During the entire flight, although short, the nose tip is ablating at a considerable rate with an expected 0.5 inch recession. The recession discussed in this context is ablation effects only. Particle impact studies will be looked at in future studies.

From Figure 3, one could assume the trajectory with the highest integrated heat flux should be the most stringent case regarding ablation effects. As expected the trajectory around the twenty degree QE has the highest total recession due to ablation of approximately 1.25 inches. On a large scale vehicle this number is small compared to the overall dimensions however on a sharp 3.6 degree cone on the order of thirty inches 1.25 inch recession is considerable (almost 5% body length). In particular the aerodynamic effects caused by the shape change will play a significant role in the guidance of the round.

Both the 50 degree QE and 85 degree QE trajectories behaved similarly to each other due to the endo-exo-endo nature of the flight. Since heat flux is a function of density gaining altitude greatly reduces the heat flux on the round. Both trajectories displayed this with a steep ablation curve initially tapering off to nothing and then upon reentry begin to recess again. Total amounts are approximately, 0.7 inches and 0.55 inches for the 50 degree and 85 degree cases respectively.

For comparison, ATAC05 was intended to be used to perform the exact same study as done with ASCC86. Unfortunately significant limitations prevented the comparison. Many of the issues outlined in the following paragraphs will be corrected in a current effort by ITT.

It was found that unlike ASCC 86, ATAC05 was relatively easy to get a solution. The major difference is that ASCC86 will not provide a solution if convergence was not obtained. However, ATAC05 will provide a solution even if there was poor convergence. Convergence studies showed many inconsistencies with the code. Three studies were done with ATAC05 in order to establish where the inconsistencies were – time step variation, stream line variation, and patch variation. Due to time constraints only a study was done on 0.125 inch nose tip. Similar trends

were found in 0.20 inch nose tip as well. Not until the nose tip was significantly increased did the inconsistencies die out.

By varying the time step one would assume that between time steps there would be some trend to convergence. For the small slender objects ATAC05 could not come to such a trend. Unlike ASCC86 which could come to a relatively stable temperature profile ATAC05 would have variations between time steps on the order of 1000 – 1500 °R (555 – 833 K). The code was unable to ever converge to a stable temperature profile. As a step further time steps were refined in order to potentially dampen out the wild variations as well as come to some converged value. Instead no convergence was ever encountered and the variations continued. The actual value, DTAR, in the code is a user defined initial time step size. Depending on how the solution is proceeding the code can vary the increments throughout the solution. Figure 12 show the temperature fluctuations. Notice the time steps of 1.0 seconds had a final temperature of 4320 °R (2400 K), 0.5 seconds was 3700°R(2055 K), 0.2 seconds was 4800 °R(2666 K), and 0.1 seconds at 5500°R(3055 K). Further reductions of an order of magnitude made no difference or trend.

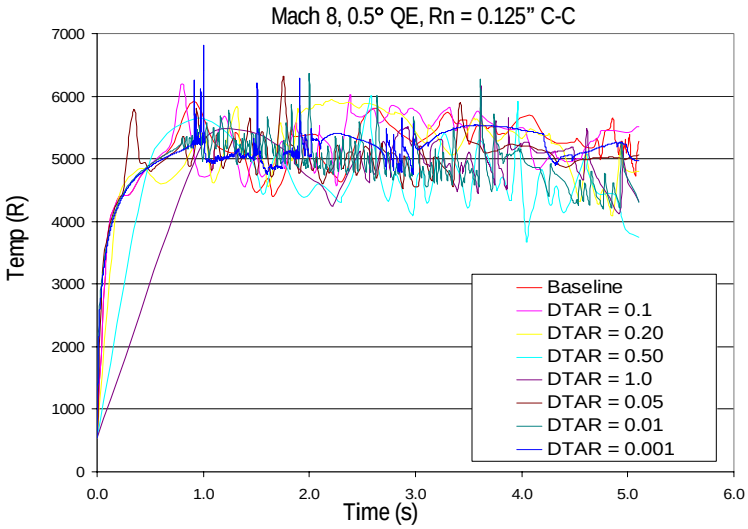

FIGURE 13: ATAC05 TEMPERATURE HISTORIES

As a result of the variations in temperature predictions the predicted recession was also inconsistent. Depending on whether that particular thermal history was higher or lower than the next time step recessions varied as much as 50%. Again as can be seen in Figure 14 there is no particular trend present as time steps are refined.

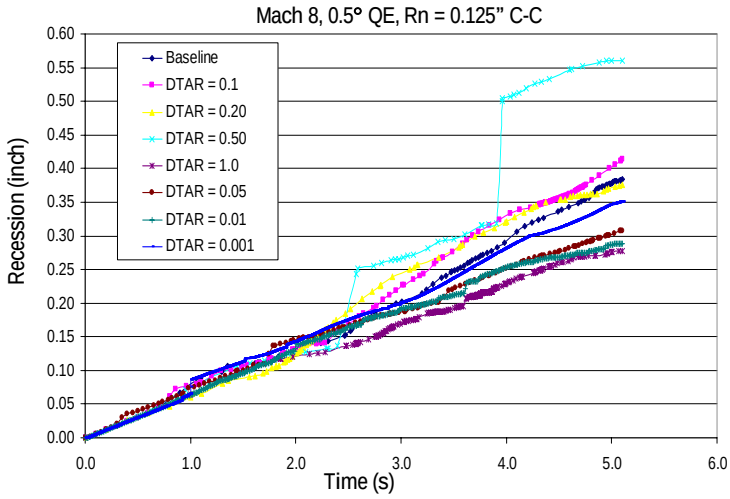

FIGURE 14: ATAC05 RECESSION

Similar studies were performed varying the number of streamlines per patch as well as number of patches on a given segment. In each of these studies similar inconsistencies were seen. The temperature fluctuations continued in all cases as before. Figures 15 through 18 show the resulting thermal histories and recession predictions for the studies.

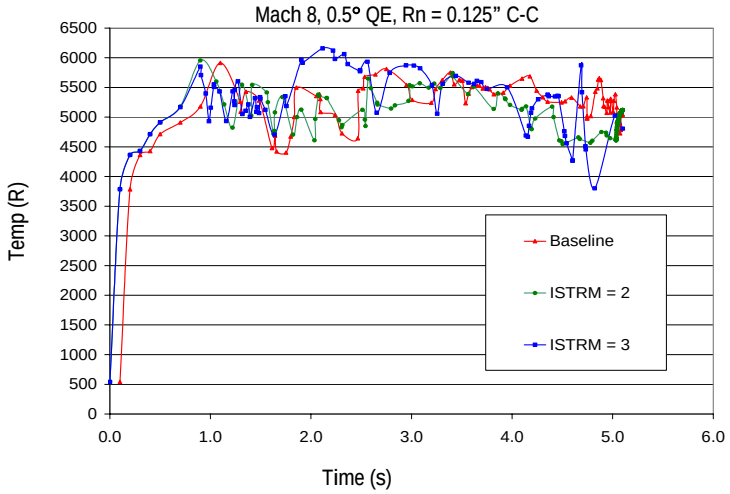

FIGURE 15: STREAMLINE VARIATIONTHERMAL HISTORY

Notice in thermal history plots, Figures 15 and 17, the temperatures are all fairly close to each other. Obviously there is still the wide variation from time step to time step but on average the results are close. In contrast the recession predictions show much more variation than alluded to by the temperature histories.

The baseline case used one streamline per patch. By increasing from one to two streamlines changes the recession solution slightly as expected. Logically increasing the streamlines even more should also result in a slight change eventually coming to some convergence. Instead increasing from two to three streamlines changes the recession significantly.

Patch variation behaved much more consistently with expectations. The baseline number of patches per segment is

four. Reducing this number to three significantly changed the recession predications. In the other direction, as the number of patches was increased – thus giving finer resolution – the recession predication tended towards a converged value.

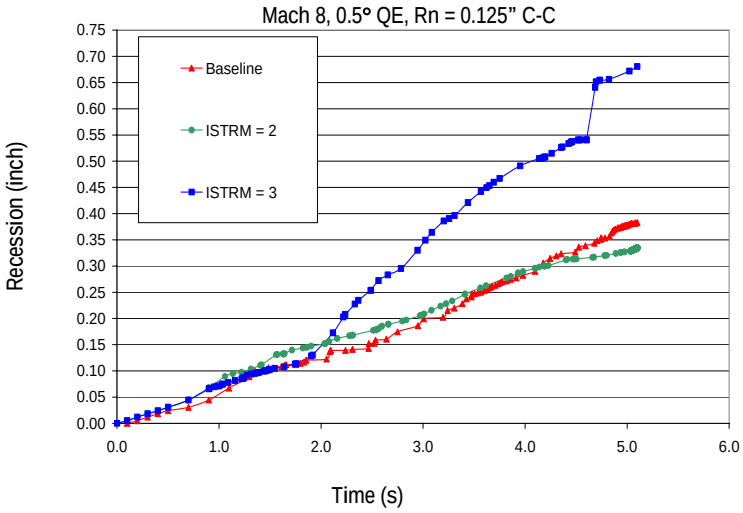

FIGURE 16: STREAMLINE VARIATION RECESSION

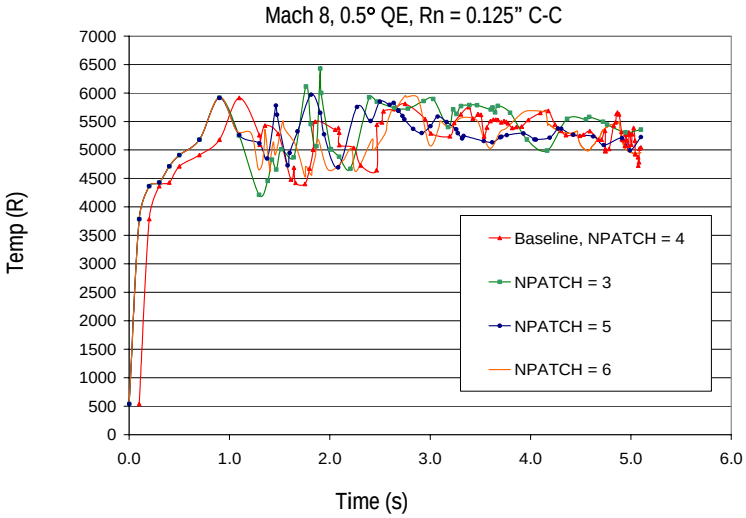

FIGURE 17: PATCH VARIATION THERMAL HISTORY

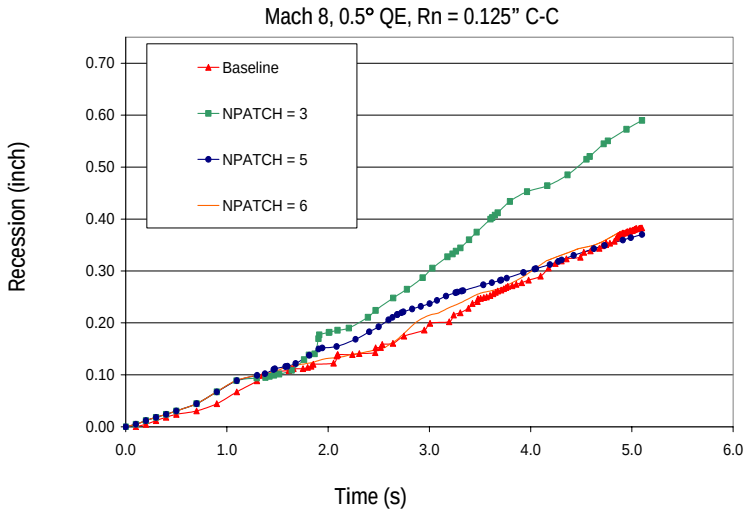

FIGURE 18: PATCH VARIATION RECESSION

Further studies need to be performed with ATAC05 in order to ascertain where the inconsistencies lie. By doing so these particular areas can be reevaluated and corrected if needed. From discussions with AMRDEC, ITT has intentions to bring some resolution to these outstanding concerns.

CONCLUSIONS

With current engineering tools available to date this study acted as a means to begin to understand the design requirements for the thermal system of a hypersonically launched sea level projectile. Temperatures in excess of 6000 °R (3000 K) are not unreasonable and are to be expected for this application. Furthermore, recession amounts on the order of 1.5 inches or more importantly almost 5% loss of the entire airframe length.

These temperatures are fairly typical of high performance reentry vehicles. The RV community has flown materials such as carbon-carbon at these temperatures with good survival rates. The major difference in this particular case is time duration for the onset of the maximum temperatures and pressures. RVs although operating at extreme velocities do not encounter significant air density for a period of time. The heating and loading profiles are much less severe than instantaneous thermal and pressure loading seen from a hypersonic sea level system. Test facilities do not have the capabilities to run at these flight conditions. Until the ability to fire these rounds at the desired sea level velocities testing will have to be piecemealed to attempt to obtain some data at close to design conditions. All conditions may not be tested at once but via arc jets, tunnels, sled track and laser facilities many of the design conditions can be approximated. The all up testing will come with a gun system capable of firing at these velocities.

All the various codes have there places within the fidelity levels necessary however there are still significant limitations. Some of the basic tools, such as BLUNTY/SODDIT, are excellent at giving quick first cut temperature and ablation predictions. They act as a sanity check before continuing with higher fidelity analyses. If used in this manner the limitations are much less limiting. From the analyses presented within this paper.

BLUNTY/SODDIT provided very similar numbers to those predicted by the higher fidelity codes. The geometric modeling scheme used and the one dimensional nature of SODDIT do limit the capabilities thus requiring the need for higher fidelity codes for more stringent design studies.

Similarly ASCC86 and ATAC05 are exceptionally useful tools. Both codes have a much broader range of applicability than BLUNTY/SODDIT however these two are not without limitations. Both codes, not surprisingly since they are built from the same original source, have geometric limitations. ASCC86 clearly shows that the gridding scheme used may not be appropriate for slender sharp bodies. Increasing the nose tip radius helped in converging the solution which also points to the geometric issues. On the other hand ATAC05 seemed to more often than not come to a solution even if it was incorrect. Nothing obviously pointed to geometric concerns but it would be a smart first place to look considering the experiences with ASCC86.

FUTURE WORK

This study was intended to develop an understanding of the currently available tools and their capabilities and limitations in this flight realm. The analyses performed gave insight to the major design issues associated with this round as well as outlined some of the long poles in the tent. Further analyses will be conducted to couple the aeroheating boundary conditions from BLUNTY and MAGIC to a full up finite element model in order to characterize the entire rounds thermal response. Understanding the operating temperatures and thermal stresses within the airframe and subassemblies will be crucial to a successful design. Secondly, due to the lack of validation and verification in this flight regime for these codes some computational fluid analyses will be performed. These data points will help bound the problem as well as provide some verification of the boundary conditions predicted in the engineering tools.

ACKNOWLEDGMENTS

The author gratefully acknowledges the Office of Naval Research for funding this effort as well as contributions made by Sandia National Laboratories (D. Potter, D. Kuntz, and B. Hassan), AMRDEC (G. Russell, B. Moylan) and ITT (F. Strobel, A. Murray). This effort also is serving for thesis work through Virginia Tech (Dr. J. Schetz advisor).

REFERENCES

1. Ellis R.L, Poyner J.C & McGlasson ' Influence of Bore and Rail Geometry on an Electromagnetic Naval Railgun System', IEEE Transactions on Magnetics, Vol. 41, January 2005.

2. Hochrein, G.J., A Procedure for Computing Aerodyanmic Heating on Sphere-Cones – Program BLUNTY, Volume 1: Concept and Results, Sandia Laboratories, Albuquerque, New Mexico, SC-DR-69-243, CFRD, June 1969.

3. Noack, R.W., Walker, M.A., Lopez, A.R. PURMAGIC: Processing Utility for Running Multiple Aerodyanmic Codes and Geometries Using an Interactive Computer, Sandia National Laboratories, Albuquerque, NM, SAND89-0561, March 1989.

4. Polansky, G.F., Hypersonic Integral Boundary Layer Analysis of Reentry Geometries (HIBLARG) Code Description and User's Manual Version 2.0, Sandia National Laboratories, Albuquerque, NM, SAND89-0552, March 1989.

5. King, HC., Muramoto, K.K., Murray, A.L., Pronchick, SW. ABRES Shape Change Code (ASCC86), Technical Report and User's Manual. AcurexCorporation, Aerotherm Division. December 1986. BMO TR-87-57.

6. Murray, A.L. Users Manual for the Aeroheating and Thermal Analysis Code (ATAC05). ITT Industries, Huntsville, AL. July 2005.

7. Aeroprediction Code 2002, Aeroprediction Inc., Moore, F.G.

8. Approximate Methods For Weapon Aerodynamics, Moore, F.G. AIAA 2000

9. Eckert, E.R.G. "Engineering Realtions for Heat Transfer and Friction in High-Velocity Laminar and Turbulent Boundary Layer Flow over Surfaces with Constant Pressure and Temperature, " Transcript of the American Socity of Mechanical Engineers, Vol. 78, No. 6, 1956.

10. Hypersonic Aerothermodynamics, Bertin, J. AIAA 1994

11. Hypersonic and High Temperature Gas Dynamics, Anderson, J.D. McGraw-Hill, 1989.